Variational Models for Dynamic Tomography

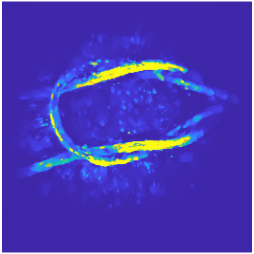

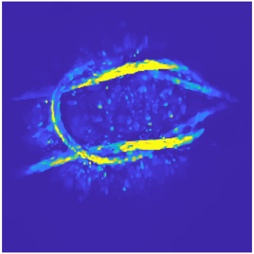

Felix Lucka
Centrum Wiskunde & Informatica
University College London
Felix.Lucka@cwi.nl

Inverse Problems: Modelling & Simulation
Malta

Joint with: S. Arridge, B. Cox, N. Huynh, M. Betcke, P. Beard & E. Zhang J. Batenburg, S. Coban, R. Lagerwerf, H. Der Sarkissian, J.W. Buurlage, G. Colacicco, M. Zeegers

May 23, 2018

Centre for Medical Image Computing

Variational Models for Dynamic Tomography

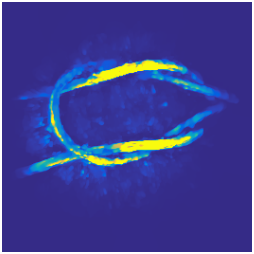

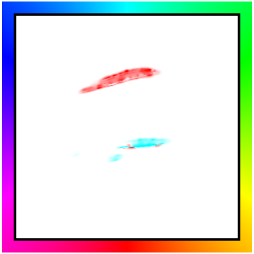

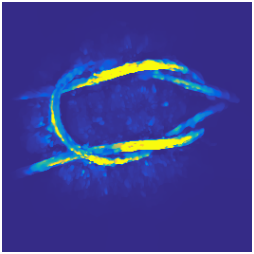

Felix Lucka
Centrum Wiskunde & Informatica
University College London
Felix.Lucka@cwi.nl

Inverse Problems: Modelling & Simulation
Malta

Joint with: S. Arridge, B. Cox, N. Huynh, M. Betcke, P. Beard & E. Zhang J. Batenburg, S. Coban, R. Lagerwerf, H. Der Sarkissian, J.W. Buurlage, G. Colacicco, M. Zeegers

May 23, 2018

Centre for Medical Image Computing

Basics of Photoacoustic Tomography (PAT)

Optical Part

optical absorption coefficient: μ_a

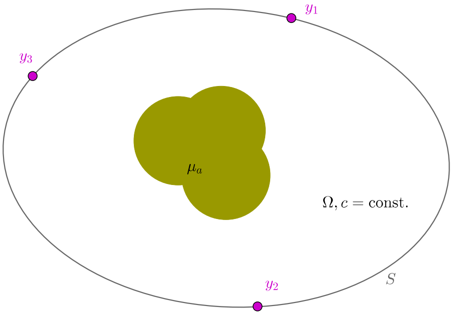

Acoustic Part

Basics of Photoacoustic Tomography (PAT)

Optical Part

optical absorption coefficient: μ_a

pulsed laser excitation: Φ

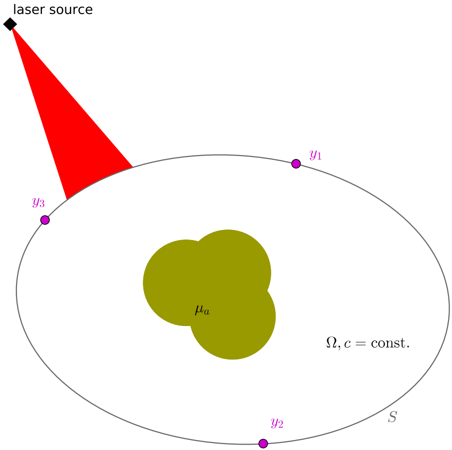

Acoustic Part

Basics of Photoacoustic Tomography (PAT)

Optical Part

optical absorption coefficient: μ_a

pulsed laser excitation: Φ

thermalization by chromophores: $H = \mu_a \Phi$

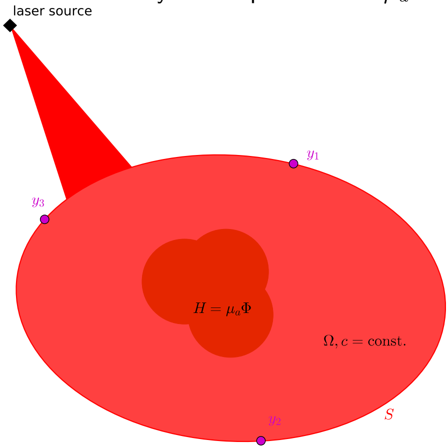

Acoustic Part

Basics of Photoacoustic Tomography (PAT)

Optical Part

optical absorption coefficient: μ_a

pulsed laser excitation: Φ

thermalization by chromophores: $H = \mu_a \Phi$

Acoustic Part

local pressure increase: $p_0 = \Gamma H$

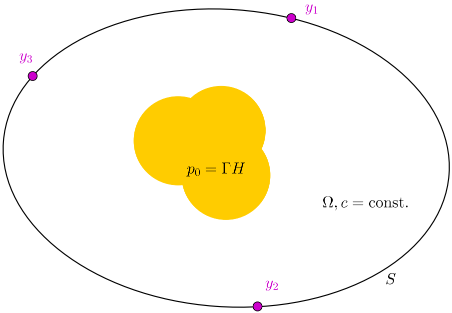

Basics of Photoacoustic Tomography (PAT)

Optical Part

optical absorption coefficient: μ_a

pulsed laser excitation: Φ

thermalization by chromophores: $H = \mu_a \Phi$

Acoustic Part

local pressure increase: $p_0 = \Gamma H$

elastic wave propagation:

$$\Delta p - \frac{1}{c^2} \frac{\partial^2 p}{\partial^2 t} = 0$$

$$p|_{t=0} = p_0, \quad \frac{\partial p}{\partial t}|_{t=0} = 0$$

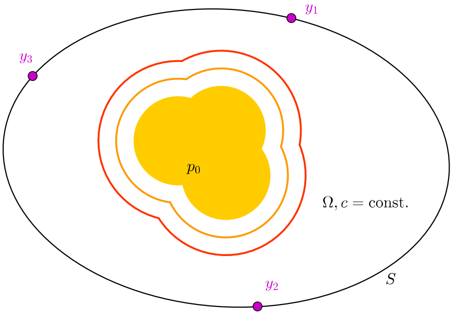

Basics of Photoacoustic Tomography (PAT)

Optical Part

optical absorption coefficient: μ_a

pulsed laser excitation: Φ

thermalization by chromophores: $H = \mu_a \Phi$

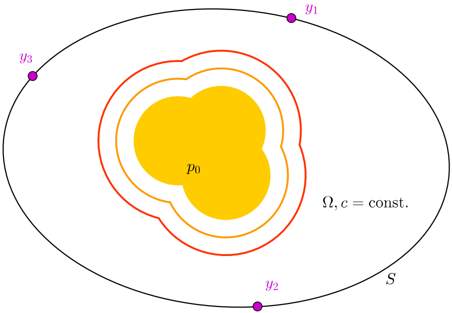

Acoustic Part

local pressure increase: $p_0 = \Gamma H$

elastic wave propagation:

$$\Delta p - \frac{1}{c^2}\frac{\partial^2 p}{\partial^2 t} = 0$$

$$p|_{t=0} = p_0, \quad \frac{\partial p}{\partial t}|_{t=0} = 0$$

measurement of pressure time courses:

$$f_i(t) = p(y_i, t)$$

Basics of Photoacoustic Tomography (PAT)

Optical Part

optical absorption coefficient: μ_a

pulsed laser excitation: Φ

thermalization by chromophores: $H = \mu_a \Phi$

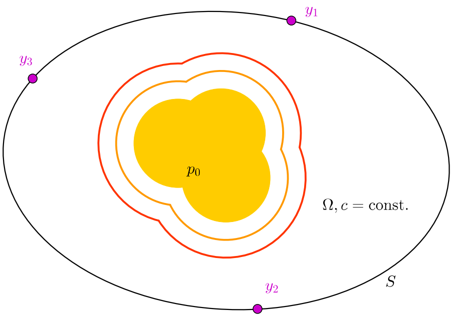

Acoustic Part

local pressure increase: $p_0 = \Gamma H$

elastic wave propagation:

$$\Delta p - \frac{1}{c^2}\frac{\partial^2 p}{\partial^2 t} = 0$$

$$p|_{t=0} = p_0, \quad \frac{\partial p}{\partial t}|_{t=0} = 0$$

measurement of pressure time courses:

$$f_i(t) = p(y_i, t)$$

Photoacoustic effect

- coupling of optical and acoustic modalities.
- "hybrid imaging"
- high optical contrast can be read by high-resolution ultrasound.

Basics of Photoacoustic Tomography (PAT)

Optical Part

optical absorption coefficient: μ_a

pulsed laser excitation: Φ

thermalization by chromophores: $H = \mu_a \Phi$

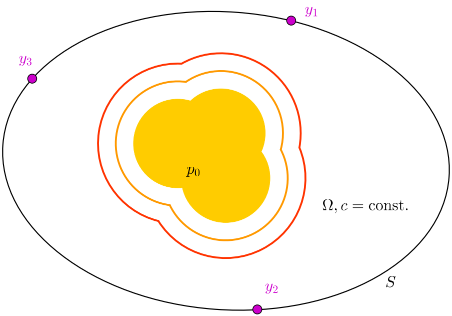

Acoustic Part

local pressure increase: $p_0 = \Gamma H$

elastic wave propagation:

$$\Delta p - \frac{1}{c^2}\frac{\partial^2 p}{\partial^2 t} = 0$$

$$p|_{t=0} = p_0, \quad \frac{\partial p}{\partial t}|_{t=0} = 0$$

measurement of pressure time courses:

$$f_i(t) = p(y_i, t)$$

Inverse problems:

! optical inversion (μ_a) from boundary data: severely ill-posed.

Basics of Photoacoustic Tomography (PAT)

Optical Part

optical absorption coefficient: μ_a

pulsed laser excitation: Φ

thermalization by chromophores: $H = \mu_a \Phi$

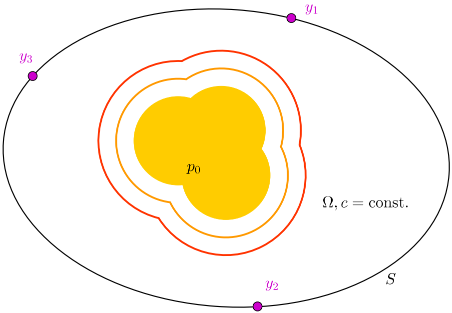

Acoustic Part

local pressure increase: $p_0 = \Gamma H$

elastic wave propagation:

$$\Delta p - \frac{1}{c^2}\frac{\partial^2 p}{\partial^2 t} = 0$$

$$p|_{t=0} = p_0, \quad \frac{\partial p}{\partial t}|_{t=0} = 0$$

measurement of pressure time courses:

$$f_i(t) = p(y_i, t)$$

Inverse problems:

- ! optical inversion (μ_a) from boundary data: severely ill-posed.
- ✓ acoustic inversion (p_0) from boundary data: moderately ill-posed.
- ✓ optical inversion (μ_a) from internal data: moderately ill-posed.

Photoacoustic Imaging: Applications

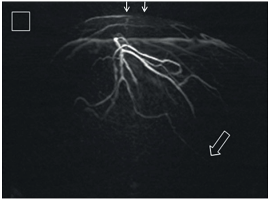

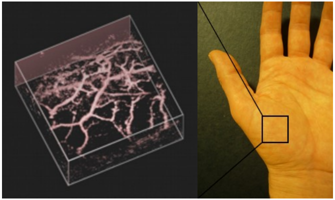

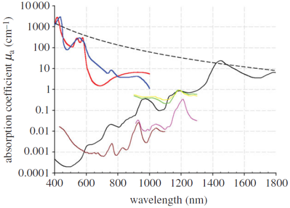

- Light-absorbing structures in soft tissue.
- High contrast between blood and water/lipid.
- Different wavelengths allow quantitative spectroscopic examinations.
- Sensitive to blood oxygen saturation (SO_2).
- Use of contrast agents for molecular imaging.
- Extremely promising future imaging technique!

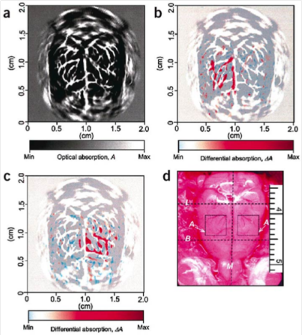

sources: **Paul Beard, 2011.** Biomedical photoacoustic imaging, Interface Focus. Wikimedia Commons

Dynamic High Resolution Photoacoustic Tomography

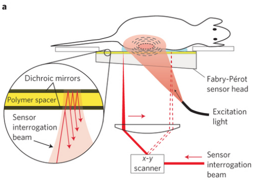

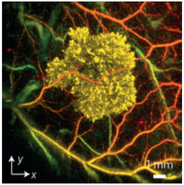

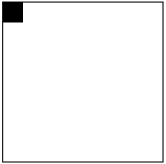

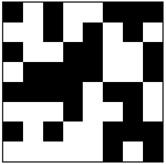

Fabry Pérot (FB) interferometer:

✓ High spatial resolution

! Nyquist sampling leads to low temporal resolution

⇝ Beat Nyquist for sparse targets by incoherent sampling of each frame/wavelength t ("compressed sensing"):

$$f_t^c = C_t f_t = C_i(Ap_t + \varepsilon_t), \qquad t = 1, \dots, T$$

Image reconstruction:

1. $f_t^c \longrightarrow f_t$, $f_t \longrightarrow p_t$ by standard method.
2. $f_t^c \longrightarrow p_t$: standard or new method?
3. $F^c \longrightarrow P$: Full spatio-temporal method.

PAT Reconstruction & Numerical Wave Propagation

Variational regularization:

$$\hat{p}_t = \underset{p \geqslant 0}{\operatorname{argmin}} \left\{ \frac{1}{2} \left\| C_t A p - f_t^c \right\|_2^2 + \lambda \mathcal{J}(p) \right\}$$

! Iterative first-order methods require implementation of A and A^*.

✓ k-space pseudospectral time domain method for 3D wave propagation:

B. Treeby and B. Cox, 2010. k-Wave: MATLAB toolbox for the simulation and reconstruction of photoacoustic wave fields, *Journal of Biomedical Optics.*

✓ Derivation and discretization of adjoint PAT operator A^*:

Arridge, Betcke, Cox, L, Treeby, 2016. On the Adjoint Operator in Photoacoustic Tomography, *Inverse Problems 32(11).*

CWI

Accelerated 3D PAT via Compressed Sensing

$$\hat{p}_t = \underset{p \geqslant 0}{\operatorname{argmin}} \left\{ \frac{1}{2} \| C_t A p - f_t^c \|_2^2 + \lambda \mathcal{J}(p) \right\}$$

- ✓ combination of compressed sensing and sparsity-constrained image reconstruction
- ✓ generic total variation (TV) regularization enhanced by Bregman iterations
- ✓ extensive evaluation with realistic numerical phantom, experimental and *in-vivo* data
- ✓ significant acceleration with minor loss of quality.
- ! frame-by-frame reconstruction, only.

Arridge, Beard, Betcke, Cox, Huynh, L, Ogunlade, Zhang, 2016. Accelerated High-Resolution Photoacoustic Tomography via Compressed Sensing, *Physics in Medicine and Biology 61(24).*

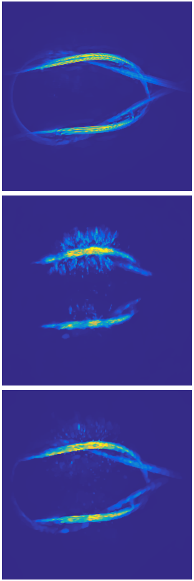

Spatio-Temporal Reconstruction (4D Tomography)

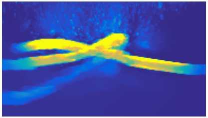

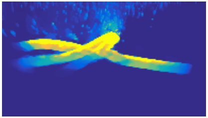

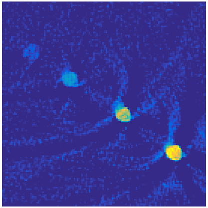

Continuous data acquisition

$\Longrightarrow$ tradeoff between spatial and temporal resolution.

Different dynamic models:

- Parametric models (shift, stretch, etc.): simple and nice if applicable.
- Structured Low-Rank (functional imaging with static anatomies/QPAT).
- Tracer uptake/wash-in models.
- Perfusion models.
- Needle guidance
- Intra-operative endoscopic imaging.
- Joint image reconstruction and motion estimation.

Spatio-Temporal Reconstruction (4D Tomography)

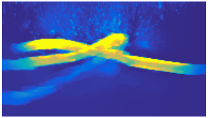

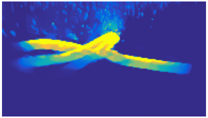

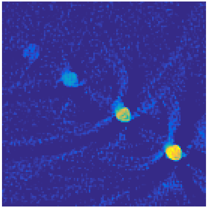

Continuous data acquisition

$\Longrightarrow$ tradeoff between spatial and temporal resolution.

Different dynamic models:

- Parametric models (shift, stretch, etc.): simple and nice if applicable.
- Structured Low-Rank (functional imaging with static anatomies/QPAT).
- Tracer uptake/wash-in models.
- Perfusion models.
- Needle guidance
- Intra-operative endoscopic imaging.
- **Joint image reconstruction and motion estimation.**

General Dynamics

$$\hat{p}_t = \underset{p \geqslant 0}{\operatorname{argmin}} \left\{ \frac{1}{2} \| C_t A p - f_t^c \|_2^2 + \lambda TV(p) \right\}, \qquad \forall\, t = 1, \ldots, T$$

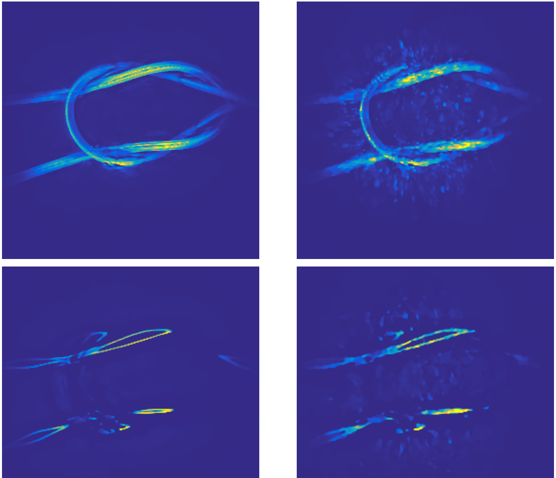

Spatio-Temporal Regularization

Non-parametric spatio-temporal regularization: Find $p \in \mathbb{R}^{N \times T}$ as

$$\hat{p} = \operatorname*{argmin}_{p \geqslant 0} \left\{ \sum_t^T \frac{1}{2} \|C_t A\, p_t - f_t^c\|_2^2 + \lambda \mathcal{R}(p) \right\},$$

Lot's of possibilities, here: Implicit model formulated as joint image and motion estimation:

$$(\hat{p}, \hat{v}) = \operatorname*{argmin}_{p \geqslant 0, v} \left\{ \sum_t^T \frac{1}{2} \|C_t A\, p_t - f_t^c\|_2^2 + \alpha \mathcal{J}(p_t) + \beta \mathcal{H}(v_t) + \gamma \mathcal{M}(p, v) \right\}$$

$\mathcal{M}(p, v)$ enforces motion PDE, e.g., optical flow equation:

$$\partial_t p(x,t) + (\nabla_x p(x,t))\, v(x,t) = 0$$

Burger, Dirks, Schönlieb, 2016. A Variational Model for Joint Motion Estimation and Image Reconstruction, *arXiv:1607.03255.*

CWI

Example: TV-TV-Lp Regularization

$$\partial_t p(x,t) + (\nabla_x p(x,t))\, v(x,t) = 0$$

$\rightsquigarrow$ discretize and penalize deviation:

$$(\hat{p},\hat{v}) = \operatorname*{argmin}_{p\geqslant 0, v} \Bigg\{ \sum_t^T \frac{1}{2} \|C_t A\, p_t - f_t^c\|_2^2$$

$$+ \alpha TV(p_t) + \beta TV(v_t) + \frac{\gamma}{p} \|(p_{t+1} - p_t) + (\nabla p_t)\cdot v_t\|_{\tilde{p}}^{\tilde{p}} \Bigg\}$$

proximal-gradient-type scheme:

$$p^{k+1} = \mathbf{prox}_{\nu\mathcal{R}} \left(p^k - \nu A^* C^* \left(C A p^k - f^c \right)\right)$$

$$\mathbf{prox}_{\nu\mathcal{R}}(q) = \operatorname*{argmin}_{p\geqslant 0} \left\{ \frac{1}{2} \|p - q\|_2^2 + \nu \mathcal{R}(p) \right\}$$

$$= \operatorname*{argmin}_{p\geqslant 0} \Bigg\{ \min_v \sum_t^T \frac{1}{2} \|p_t - q_t\|_2^2$$

$$+ \nu\alpha TV(p_t) + \nu\beta TV(v_t) + \frac{\nu\gamma}{\tilde{p}} \|(p_{t+1} - p_t) + (\nabla p_t)\cdot v_t\|_{\tilde{p}}^{\tilde{p}} \Bigg\}$$

Non-smooth Biconvex Optimization

For $\tilde{p} \geqslant 1$, TV-TV-L$\tilde{p}$ denoising is a biconvex optimization problem:

$$\min_{p \geqslant 0, v} \mathcal{S}(p,v) := \min_{p \geqslant 0, v} \sum_t^T \frac{1}{2} \|p_t - q_t\|_2^2$$
$$+ \nu\alpha TV(p_t) + \nu\beta TV(v_t) + \frac{\nu\gamma}{\tilde{p}} \|(p_{t+1} - p_t) + (\nabla p_t) \cdot v_t\|_{\tilde{p}}^{\tilde{p}}$$

Alternating optimization:

$$p^{k+1} = \operatorname*{argmin}_p \mathcal{S}(p, v^k) \qquad \text{(TV-transport constr. denoising)}$$
$$v^{k+1} = \operatorname*{argmin}_v \mathcal{S}(p^{k+1}, v) \qquad \text{(TV constr. optical flow estimation)}$$

! Both problems are convex but non-smooth.

! Need to ensure energy decrease.

Non-smooth Biconvex Optimization

Alternating optimization:

$$p^{k+1} = \operatorname*{argmin}_{p} \mathcal{S}(p, v^k) \qquad \text{(TV-transport constr. denoising)}$$

$$v^{k+1} = \operatorname*{argmin}_{V} \mathcal{S}(p^{k+1}, v) \qquad \text{(TV constr. optical flow estimation)}$$

Primal-dual hybrid gradient for both: Too slow convergence in 3D.

Alternating directions method of multipliers (ADMM):

- ! More difficult to parameterize (to ensure monotone energy).
- ! Badly conditioned, large-scale least-squares problems.
- ! Crucial: Choice of iterative solver, preconditioning and stop criterion.
- ✓ Overrelaxed ADMM with step size adaptation and CG solver for p.
- ✓ Overrelaxed ADMM with AMG-CG solver for v (frame-by-frame).
- ✓ Warm-start wherever possible.

Chambolle, Pock, 2016. An introduction to continuous optimization for imaging, *Acta Numerica.*

A 2D Example: Frame-by-Frame Least Squares

$$\hat{p}_t = \underset{p \geqslant 0}{\operatorname{argmin}} \left\{ \| C_t A p - f_t^c \|_2^2 \right\} \quad \forall\, t = 1, \ldots, T$$

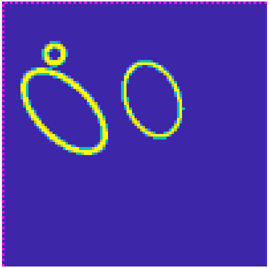

phantom

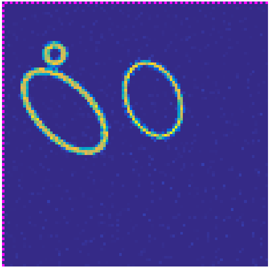

full data

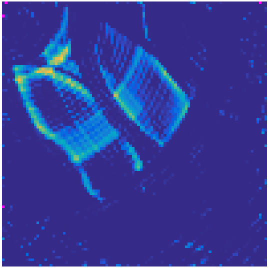

sub-sampled (25x)

A 2D Example: Frame-by-Frame Total Variation

$$\hat{p}_t = \underset{p \geqslant 0}{\operatorname{argmin}} \left\{ \| C_t A p - f_t^c \|_2^2 + \lambda TV(p) \right\} \quad \forall\, t = 1, \ldots, T$$

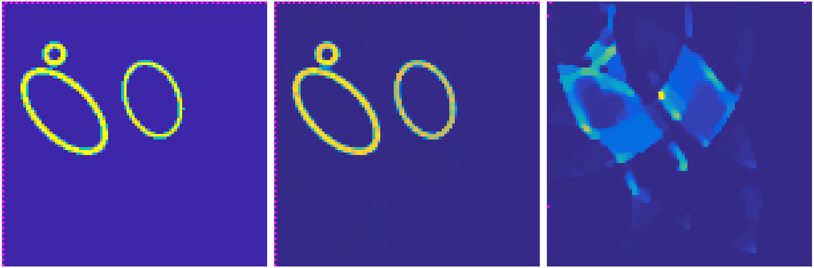

phantom | full data | sub-sampled (25x)

A 2D Example: TV-TV-L2

$$(\hat{p}, \hat{v}) = \operatorname*{argmin}_{p \geqslant 0, v} \left\{ \frac{1}{2} \sum_{t}^{T} \| C_t A \, p_t - f_t^c \|_2^2 \right.$$

$$\left. + \alpha TV(p_t) + \beta TV(v_t) + \frac{\gamma}{2} \| (p_{t+1} - p_t) + \nabla p_t \cdot v_t \|_2^2 \right\}$$

$\alpha = \beta = \lambda_{TV}$, $\gamma = 1$

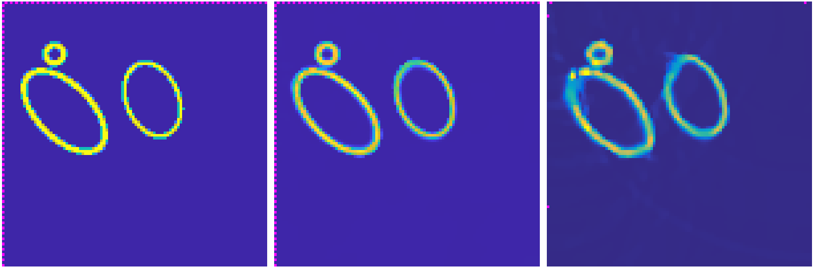

phantom | full data | sub-sampled (25x)

A 2D Example: TV-TV-L2

$$(\hat{p}, \hat{v}) = \underset{p \geqslant 0, v}{\operatorname{argmin}} \left\{ \frac{1}{2} \sum_{t}^{T} \| C_t A \, p_t - f_t^c \|_2^2 \right.$$
$$\left. + \alpha TV(p_t) + \beta TV(v_t) + \frac{\gamma}{2} \| (p_{t+1} - p_t) + \nabla p_t \cdot v_t \|_2^2 \right\}$$

$\alpha = \beta = \lambda_{TV}, \, \gamma = 0.1$

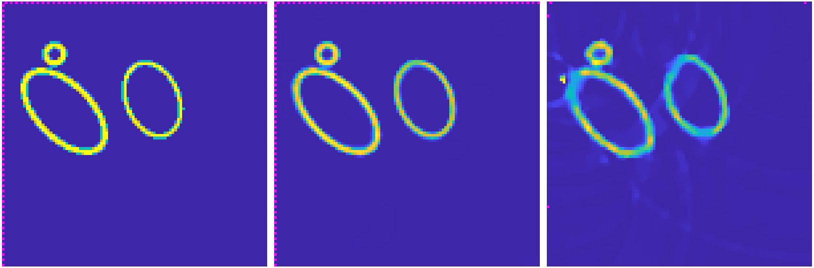

phantom full data sub-sampled (25x)

A 2D Example: Motion Estimation with TV-TV-L2

phantom

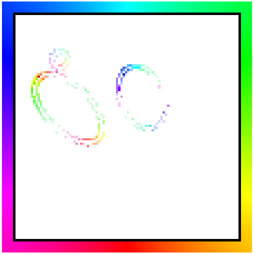

full data

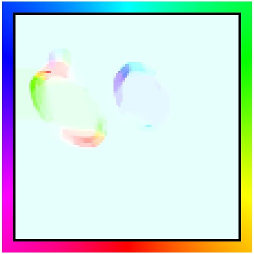

sub-sampled (25x)

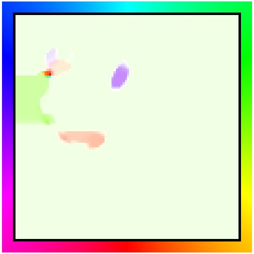

$\gamma = 1.0$

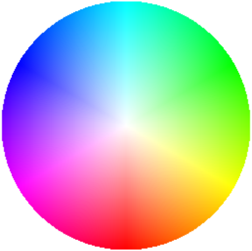

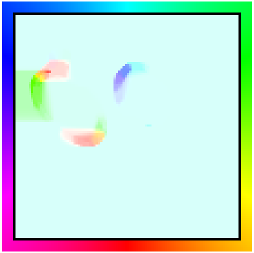

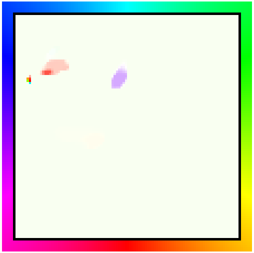

$\gamma = 0.1$

Artificially Sub-Sampled 3D Stop-Motion Data

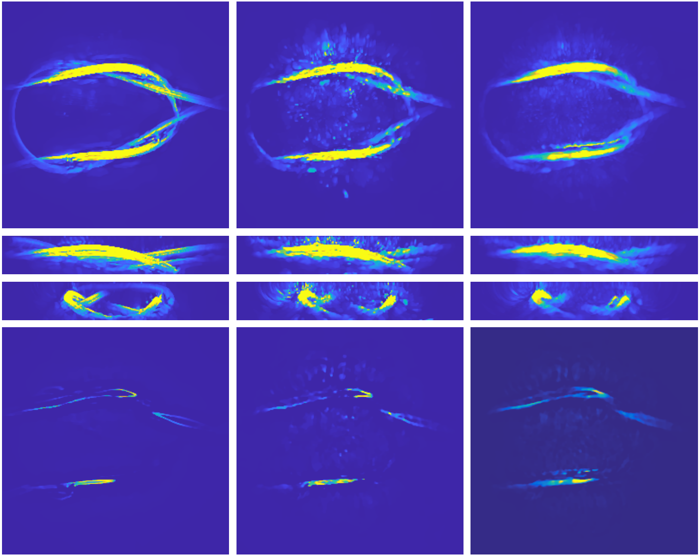

X maxIP

Y maxIP

Z maxIP

X slice

full data, TV-FbF | 16x, TV-FbF | 16x, TVTVL2, $\alpha, \beta = \lambda_{TV}, \gamma = 0.1$

Artificially Sub-Sampled 3D Stop-Motion Data

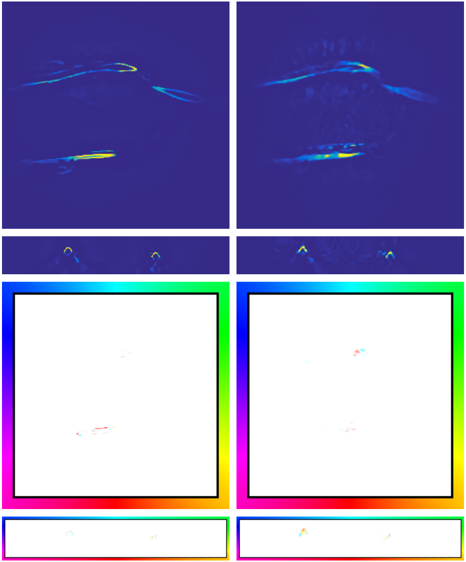

u - X slice

u - Z slice

$v - \bar{v}$ - X slice

$v - \bar{v}$ - Z slice

full data, TVTVL2 | 16x, TVTVL2

$\alpha, \beta = \lambda_{TV}, \gamma = 0.1$

Real Sub-Sampled Dynamic 3D Data (8 Beam Scanner)

sub-average over 8 frames

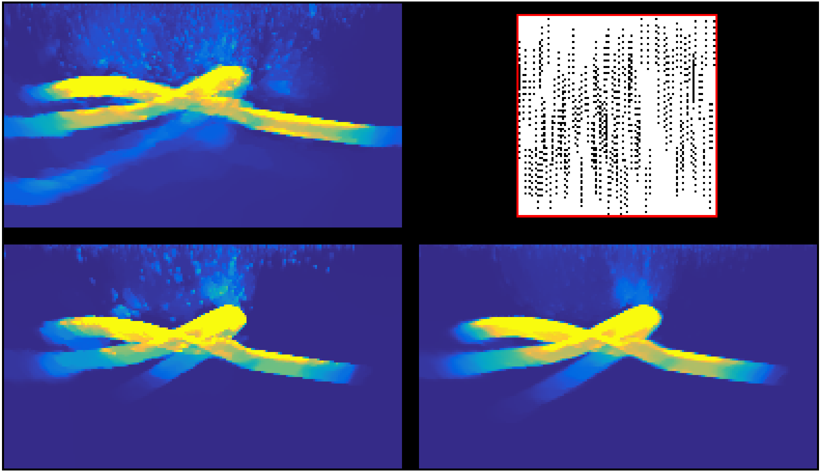

TV-FbF

TVTVL2, $\alpha = \beta = \lambda_{TV}$, $\gamma = 0.1$

In-Vivo Data: Work in Progress

human finger under various conditions (movement, arterial occulsion, thermal stimuli)

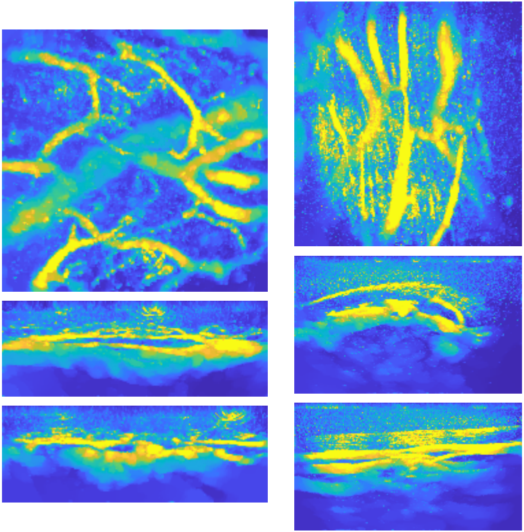

X-Ray Tomography: Interior Information from Projections

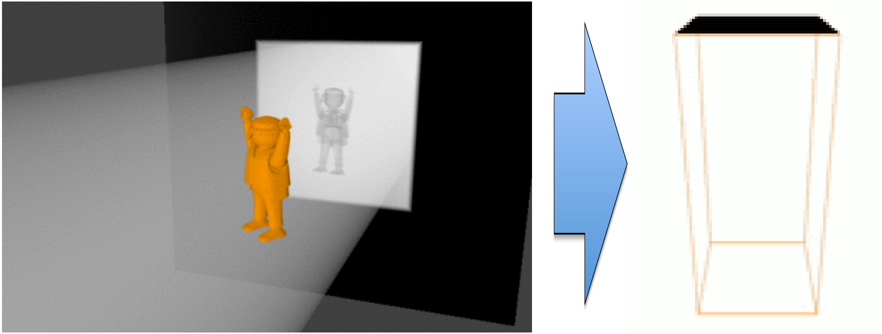

- X-rays (high-energy photons) get attenuated by matter
- 3D attenuation image from of 2D projections for different angles

FleX-ray Scanner Imaging Lab

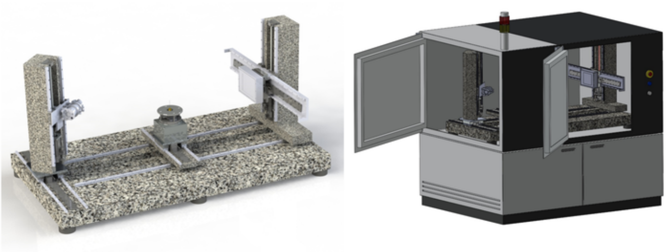

- custom-made, fully-automated CT scanner
- flexible 10 motors, individually programmable
- linked to large-scale computing hardware
- real-time adaptive 3D imaging

Dynamic CT (4D) in the FleX-ray Scanner

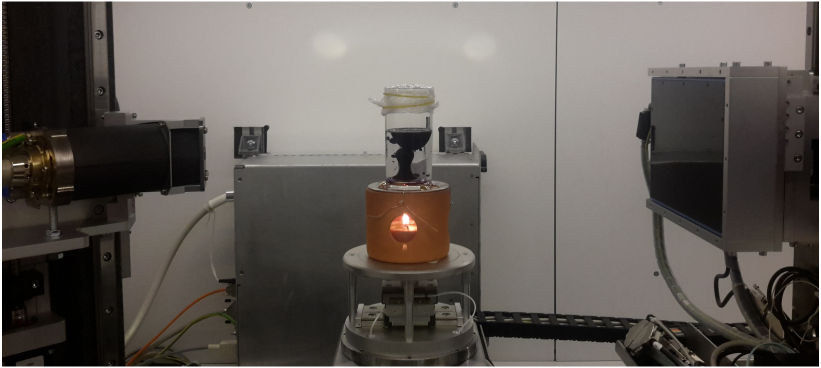

- 120 projections per rotation $\rightarrow$ each projection averaged over 3°.
- 40ms exposure per projection $\rightarrow$ 4.8s per rotation.

CWI

Summary

Photoacoustic Tomography

- Imaging with laser-generated ultrasound ("hybrid imaging")
- High contrast for light-absorbing structures in soft tissue.

Challenges of fast, high resolution 4D PAT:

- Nyquist requires several thousand detection points $\rightsquigarrow$ slow.
- High computational load.

Acceleration through sub-sampling:

- Exploit low spatio-temporal complexity to beat Nyquist.
- Acceleration by sub-sampling the incident wave field to maximize non-redundancy of data.
- Sparse, spatio-temporal variational regularization: promising results, joint estimation of dynamic parameters?

Dynamic X-Ray Tomography:

- Challenging sub-sampling scheme.
- More computational results next time!

- **L, Huynh, Betcke, Zhang, Beard, Cox, Arridge, 2018.** Enhancing Compressed Sensing Photoacoustic Tomography by Simultaneous Motion Estimation, *arXiv:1802.05184.*
- **Huynh, L, Zhang, Betcke, Arridge, Beard, Cox, 2017.** Sub-sampled Fabry-Perot photoacoustic scanner for fast 3D imaging, *Proc. SPIE 2017.*
- **Arridge, Beard, Betcke, Cox, Huynh, L, Ogunlade, Zhang, 2016.** Accelerated High-Resolution Photoacoustic Tomography via Compressed Sensing, *Physics in Medicine and Biology 61(24).*
- **Arridge, Betcke, Cox, L, Treeby, 2016.** On the Adjoint Operator in Photoacoustic Tomography, *Inverse Problems 32(11).*

cmic Centre for Medical Image Computing
EPSRC Engineering and Physical Sciences Research Council
NWO
FAMOS new lasers better diagnosis transforming healthcare
k-Wave
NVIDIA

We gratefully acknowledge the support of NVIDIA Corporation with the donation of the Tesla K40 GPU used for this research.

Thank you for your attention!

- **L, Huynh, Betcke, Zhang, Beard, Cox, Arridge, 2018.** Enhancing Compressed Sensing Photoacoustic Tomography by Simultaneous Motion Estimation, *arXiv:1802.05184.*
- **Huynh, L, Zhang, Betcke, Arridge, Beard, Cox, 2017.** Sub-sampled Fabry-Perot photoacoustic scanner for fast 3D imaging, *Proc. SPIE 2017.*
- **Arridge, Beard, Betcke, Cox, Huynh, L, Ogunlade, Zhang, 2016.** Accelerated High-Resolution Photoacoustic Tomography via Compressed Sensing, *Physics in Medicine and Biology 61(24).*
- **Arridge, Betcke, Cox, L, Treeby, 2016.** On the Adjoint Operator in Photoacoustic Tomography, *Inverse Problems 32(11).*

cmic Centre for Medical Image Computing
EPSRC Engineering and Physical Sciences Research Council
NWO
FAMOS new lasers better diagnosis transforming healthcare
k-Wave
NVIDIA

We gratefully acknowledge the support of NVIDIA Corporation with the donation of the Tesla K40 GPU used for this research.

PDHG & ADMM in 2D & 3D

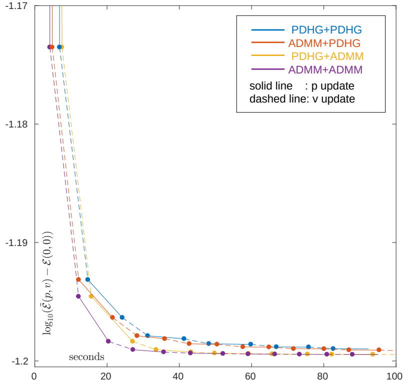

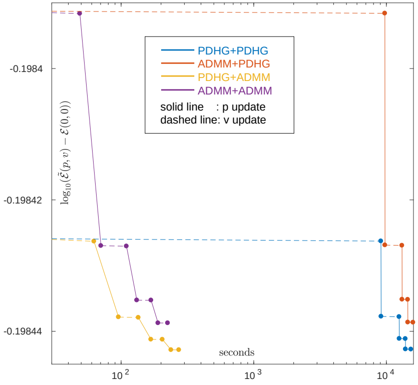

Preconditioning of the Least Squares Problem in ADMM